Electronic Supplementary Information

Novel Imine-linked Porphyrin Covalent Organic Frameworks with Good Adsorption Removing Property of RhB

Yuxia Hou, Xiaomei Zhang, Chiming Wang, Dongdong Qi, Yongqing Gu,

Ziqian Wang, and Jianzhuang Jiang*

Measurements

^{1}H NMR spectra (^{1}H-400 MHz) were recorded on a Bruker DPX 400 spectrometer in $CDCl_3$. Spectra were referenced internally using the residual solvent resonances relative to $SiMe_4$. Solid-state NMR experiments were performed on a Bruker Avance III 400 MHz spectrometer. The ^{13}C CP/TOSS NMR spectra were recorded with a 4 mm MAS probe and with a sample spinning rate of 3.0 kHz. Elemental analyses were carried out with an Elementary Vario El. IR spectra were recorded as KBr pellets using a Bruker Tensor 37 spectrometer with 2 cm^{-1} resolution. MALDI-TOF mass spectra were taken on a Bruker BIFLEX III ultra-high resolution Fourier transform ion cyclotron resonance (FT-ICR) mass spectrometer with α-cyano-4-hydroxycinnamic acid as the matrix. Powder X-ray diffraction (PXRD) data were collected on a Shimadzu XRD-6000 diffractometer using Cu-Ka radiation (I = 1.54056 Å) at room temperature. High-resolution transmission electron microscopy (HR-TEM) images were measured on a JEOL JEM-2100 electron microscope operated at 200 kV. Scanning electron microscopy (SEM) images and EDX spectra were obtained using a JEOL JEM-6510A scanning electron microscopy. For TEM imaging, a drop of freshly prepared sample solution was cast onto a carbon-coated grid. For SEM imaging, a drop of freshly prepared sample solution was cast onto a silicon slice, and then Au (1-2 nm) was sputtered onto the grids to prevent charging effects and to improve the image clarity. N_2 adsorption-desorption isotherms were measured on a QuadraSorb SI apparatus at 77 K and the surface areas of the CuP-

DMNDA-COF were calculated by the Brunauer–Emmett–Teller (BET) method. Electronic absorption spectra were recorded on a Hitachi U-4100 spectrophotometer.

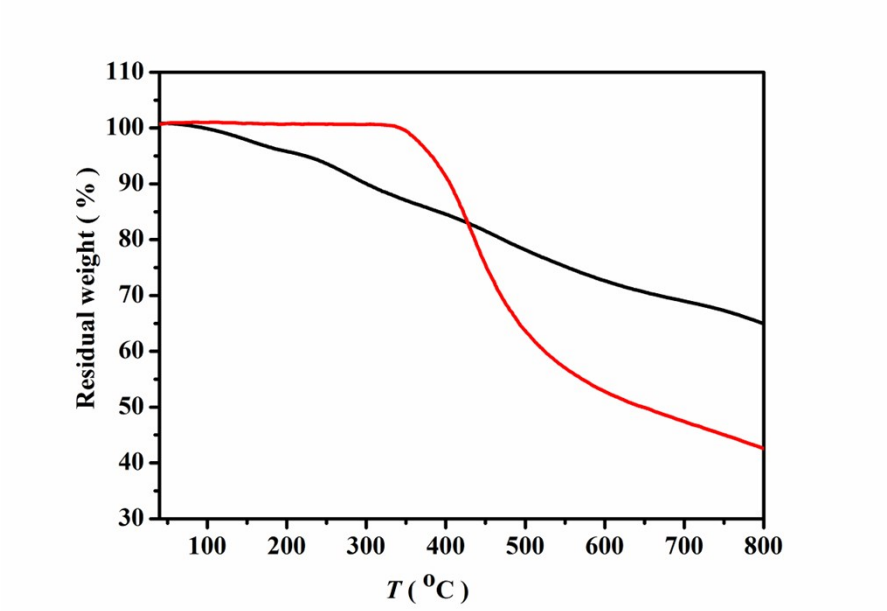

Fig. S1 Thermogravimetric analysis (TGA) data of **CuP-DMNDA-COF** (red) and **CuP-DMNDA-COF/Fe** (black).

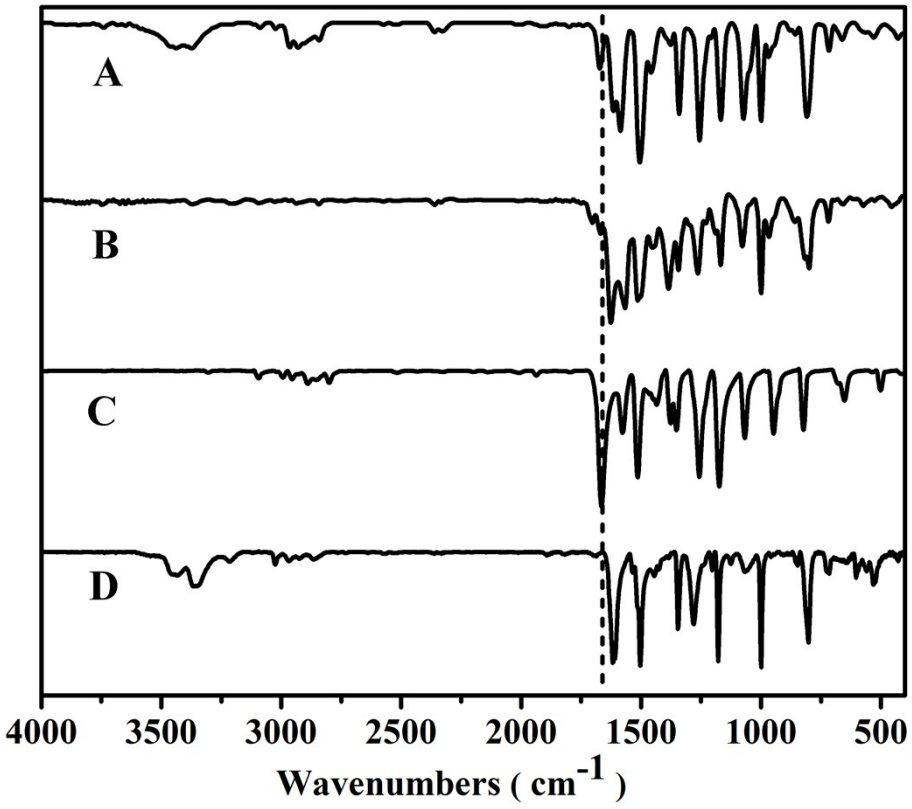

Fig. S2 FT-IR spectra of **CuP-DMNDA-COF** (A) and **CuP-DMNDA-COF/Fe** (B), DMNDA (C), and CuTAPP (D).

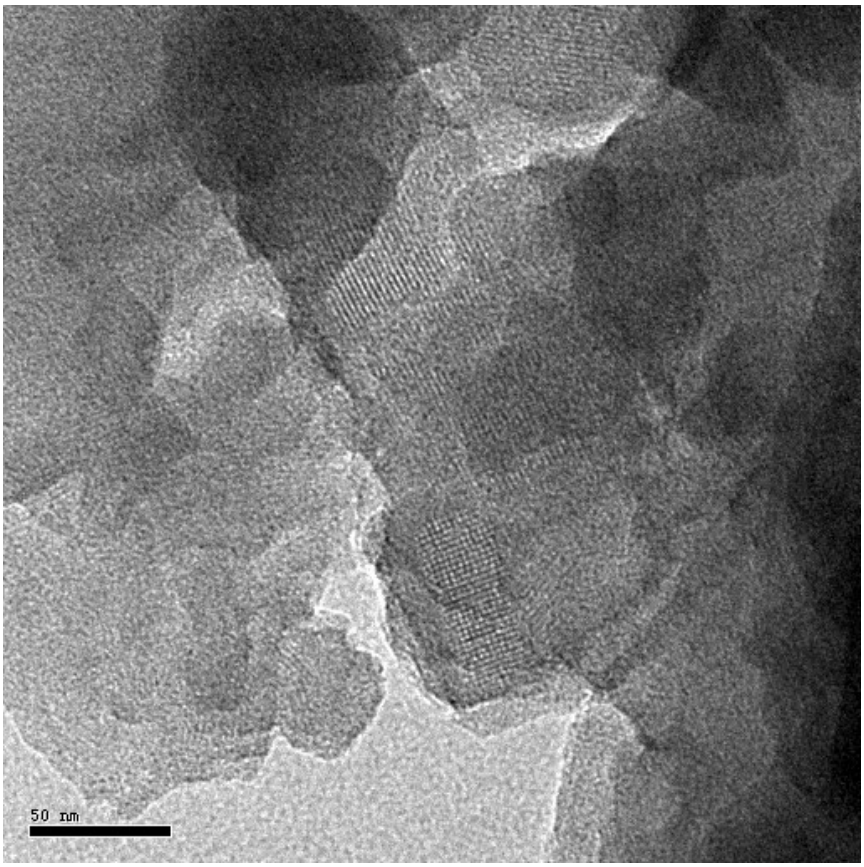

Fig. S3 TEM images of **CuP-DMNDA-COF**

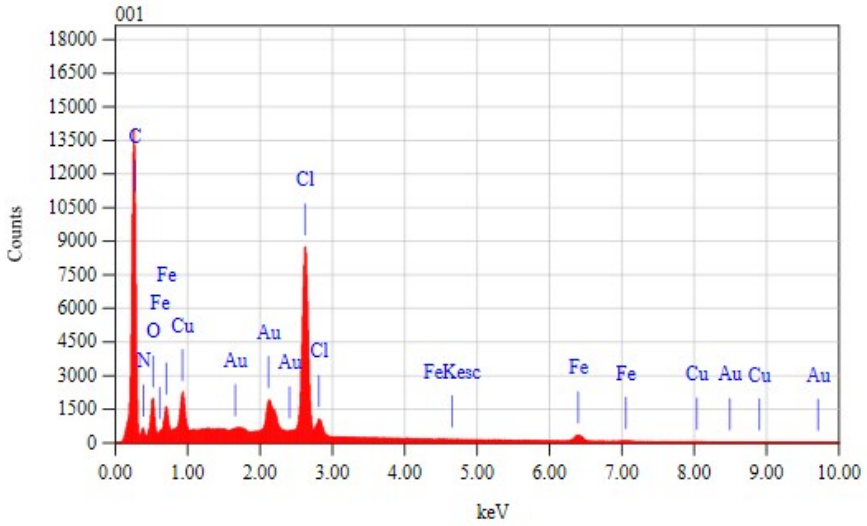

Fig. S4 Electron dispersive spectroscopy (EDS) of **CuP-DMNDA-COF/Fe**.

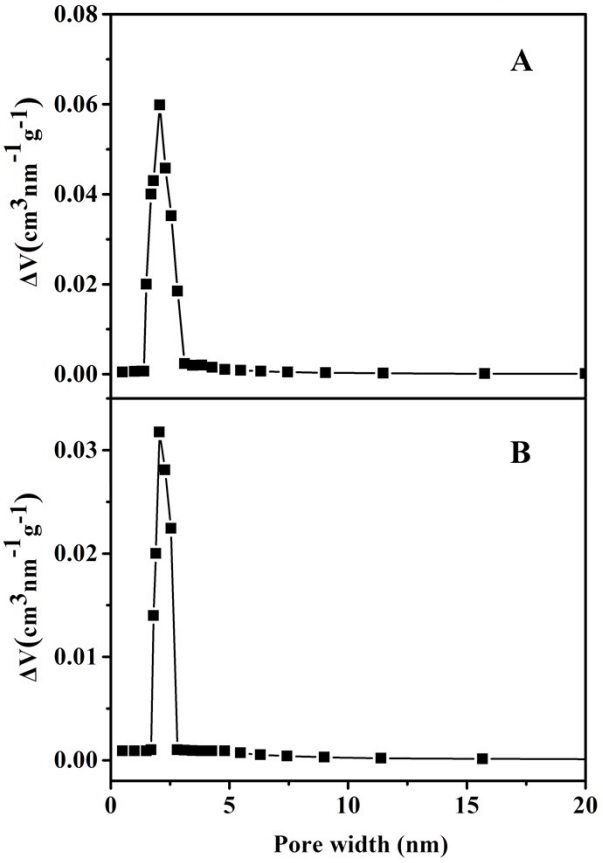

Fig. S5 Pore size distribution of **CuP-DMNDA-COF (A) and CuP-DMNDA-COF/Fe (B)**.

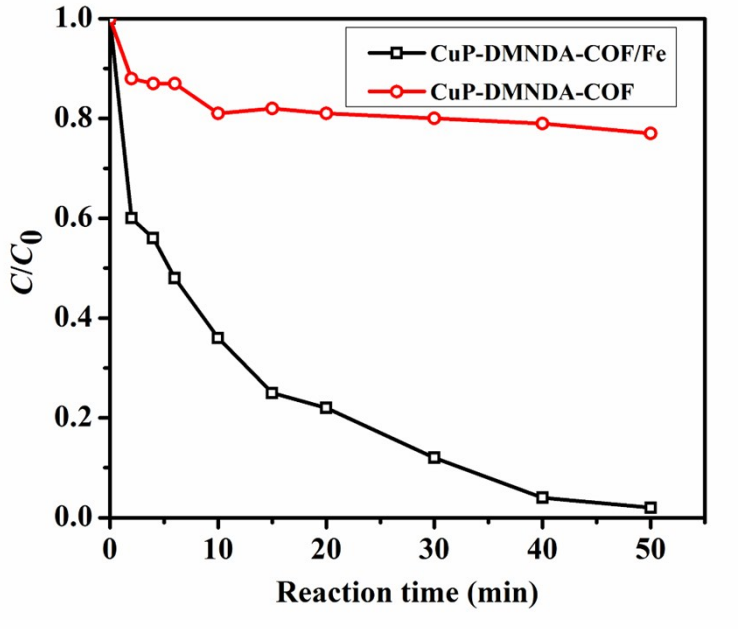

Fig. S6 The removal efficiency of **CuP-DMNDA-COF/Fe** (black) and **CuP-DMNDA-COF** (Red).

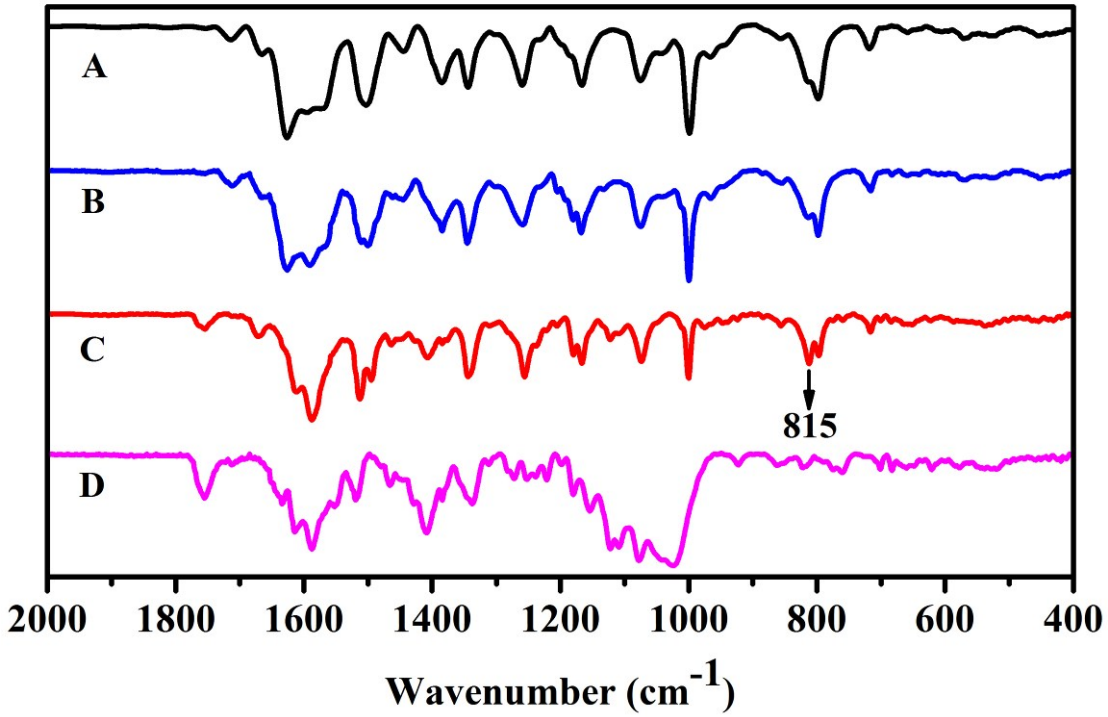

Fig. S7 FT-IR spectra of **CuP-DMNDA-COF/Fe** (A) and the mixture of **CuP-DMNDA-COF/Fe** and RhB (B), the RhB-treated **CuP-DMNDA-COF/Fe** (C), and RhB (D).

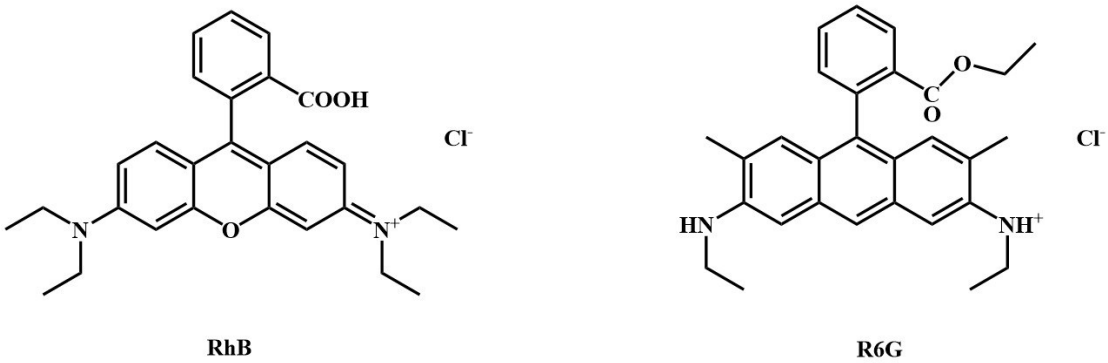

Fig. S8 The structures of dyes RhB and R6G.

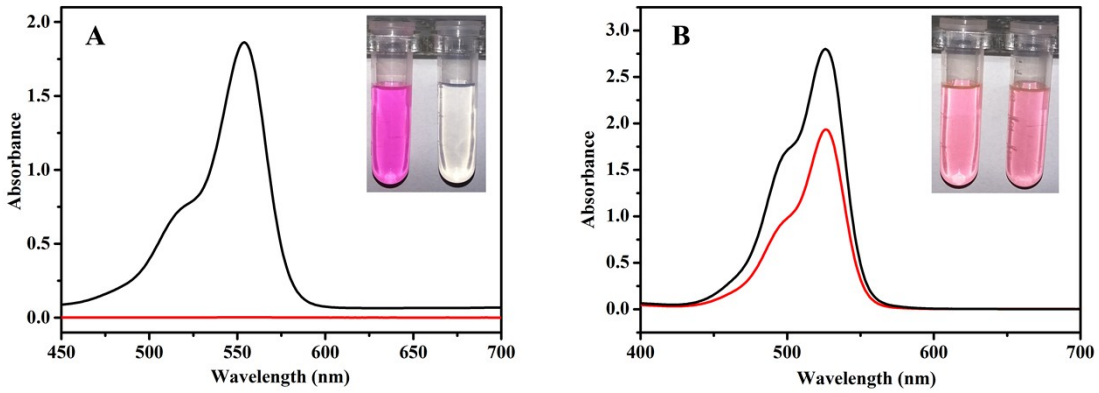

Fig. S9 Change in the UV-Vis spectra of RhB (A) and R6G (B) aqueous solution after the adsorption experiments over **CuP-DMNDA-COF/Fe** together with corresponding photographs.

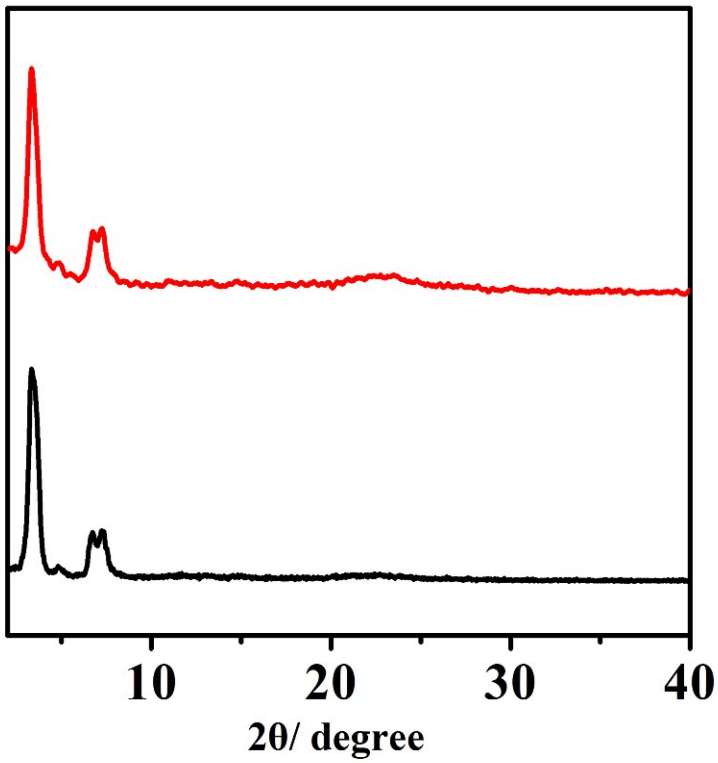

Fig. S10 PXRD patterns for **CuP-DMNDA-COF/Fe** before (black) and after (red) adsorption.

Table S1 Adsorption capacities for RhB on various porous materials.

Material	Absorption capacity for RhB [mg/g]	Ref.
CuP-DMNDA-COF/Fe	378（20°C）	This work
	424（30°C）	This work
	429（40°C）	This work
Gg-cl-P(AA-co-AAm)/Fe_3O_4	654（45°C）	1
MPGC-900	73	2
CA400	151	3
FeMB	168	4
SA/HEC/HA Membrane	18	5
C_carnauba_$CaCl_2$	39	6
Fe_3O_4/RGO(M2)	142	7
Hypercross-linked polymeric adsorbent	2	8
Iron-pillared bentonite	98	9
Poly(glutamic acid)	390	10

References

[1] H. Mittal, S. B. Mishra, Carbohydrate Polymers 101 (2014) 1255-1264.

[2] L. Sun, C. Tian, L. Wang, J. Zou, G. Mu, H. Fu, J. Mater. Chem. 21 (2011) 7232-

7239.

[3] Y. Lin, C. Chang, Separation and Purification Technology 149 (2015) 74-81.

[4] Y. Gao, Y. Guo, H. Zhang, Journal of Hazardous Materials 302 (2016) 105-113.

[5] S. S. Shenvi, A. M. Isloor, A. F. Ismail, S. J. Shilton, A. A. Ahmed, Ind. Eng. Chem. Res. 54 (2015) 4965−4975.

[6] V. S. Lacerda, J. B. López-Sotelo, A. Correa-Guimarães, S. Hernández-Navarro , M. Sánchez-Báscones, L. M. Navas-Gracia, P. Martín-Ramos, J. Martín-Gil, Journal of Environmental Management 155 (2015) 67-76.

[7] Y. Qin, M. Long, B. Tan, B. Zhou, Nano-Micro Lett. 6 (2014) 125-135.

[8] J. H. Huang, K. L. Huang, S. Q. Liu, T. Wang, C. Yan, Colloids and Surfaces A: Physicochemical and EngineeringAspects, 330 (2008) 55-61.

[9] M. F. Hou, C. X. Ma, W. D. Zhang, X. Y. Tang, Y. N. Fan, H. F. Wan, Journal of Hazardous Materials, 186 (2011) 1118-1123.

[10] B. S. Inbaraj, J. T. Chien, G. H. Hob, J. Yang, B. H. Chen, Biochemical Engineering Journal 31 (2006) 204-215.